

Short Communication

Study on the $\text{Li}_{1-x}\text{Ni}_{0.5}\text{Mn}_{1.5}\text{O}_4$ for Lithium Ion Batteries: a First-Principles Theory

Haiyan Chen^{1,2}, Lingxiao Lan^{2,*}, Meihong Huang², Xinghua Liang², Yuchao Zhao², Fawei Tang³

¹ School of Materials and Energy, Guangdong University of Technology, Guangzhou 510006, China.

² Guangxi Key Laboratory of Automobile Components and Vehicle Technology, Guangxi University of Science and Technology, Liuzhou 545006, China.

³ College of Material Science and Engineering, Beijing university of Technology, Beijing 100124, China.

*E-mail: LXH304@aliyun.com

Received: 17 February 2017 / Accepted: 4 October 2017 / Published: 12 November 2017

The crystal structure, voltage and capacity of $\text{Li}_{1-x}\text{Ni}_{0.5}\text{Mn}_{1.5}\text{O}_4$ were studied by using the first principle theory. The results show that the structure of $\text{Li}_{1-x}\text{Ni}_{0.5}\text{Mn}_{1.5}\text{O}_4$ has changed, and the lattice parameter decreased from 8.342 Å to 8.247 Å with the decrease of Li content. But the change in each direction is the same, so the octahedral structure is unchanged in the process of de-lithium. The length of Ni-O and Mn-O bonds decreases with the increase of de-lithium. The Mn-O bond decreases from 2.101 Å to 1.911 Å, while the Ni-O bond decreases from 2.065 Å To 1.965 Å. The total energy decrease from -28731.220 eV to -27178.422 eV, and the voltage decreased from 4.7 V to 4.3 V with the reduction of Li amount. All the formation energy of $\text{Li}_{1-x}\text{Ni}_{0.5}\text{Mn}_{1.5}\text{O}_4$ (P4₃32) is negative, which display that the structure of crystal is stable with no phase separation. The theoretical capacity reduced from 146 mAhg⁻¹ to 0 with the increase of delithiated amount or Li/Mn molar ratio.

Keywords: $\text{Li}_{1-x}\text{Ni}_{0.5}\text{Mn}_{1.5}\text{O}_4$, first-principles, formation energy, delithiated

1. INTRODUCTION

Lithium-ion batteries have been paid close attention by people for it has many advantages such as environment-friendly, high voltage, high energy density, large capacity and safety [1-2]. Compared with LiCoO_2 and LiMn_2O_4 , $\text{LiNi}_{0.5}\text{Mn}_{1.5}\text{O}_4$ is a good choice for secondary due to its non-toxicity, low cost and high voltage platform. It has been well known that $\text{LiNi}_{0.5}\text{Mn}_{1.5}\text{O}_4$ has a 146.7 mAhg⁻¹ capacity, and the charge/discharge voltage platform of $\text{LiNi}_{0.5}\text{Mn}_{1.5}\text{O}_4$ spinel material is about 4.7 V

[3-7], therefore it deserves to be studied by people as a kind of cathode materials for new-generation lithium-ion batteries [8-9]. Generally people improve the electrochemical performance of spinel $\text{LiNi}_{0.5}\text{Mn}_{1.5}\text{O}_4$ by using other transition metal ion to substitute Mn sites [10-11]. Ni, Co, Mg, Fe, Li, and Al are the main elements among these dopant elements [12-14]. People usually use other methods to replace the experimental method to carry out the research for experiment costs too much and the step so many that it is easy to affect the accuracy of the results [15]. In recent years, in order to analyze the cause of the essence of this phenomenon, many people are keen to study its microstructure, density of states, charge density and other properties using the first-principles [16]. The study of high potential lithium battery cathode material $\text{LiNi}_{0.5}\text{Mn}_{1.5}\text{O}_4$ mainly concentrated in the phase variable electronic structure and doping context using first-principles [17]. $\text{LiNi}_{0.5}\text{Mn}_{1.5}\text{O}_4$ have two different structures, that is Fd-3m and $P4_332$ space group. In this paper, we chose $P4_332$ space group as the research object due to its structure is more stable than Fd-3m. This paper study mainly on the crystal structure, intercalation voltage and capacity of $\text{Li}_{1-x}\text{Ni}_{0.5}\text{Mn}_{1.5}\text{O}_4$ ($P4_332$) by means of first-principles theory. Meanwhile, we discussed the impact of these properties on their electrochemical properties such as structural stability and electronic conductivity.

2. METHODS

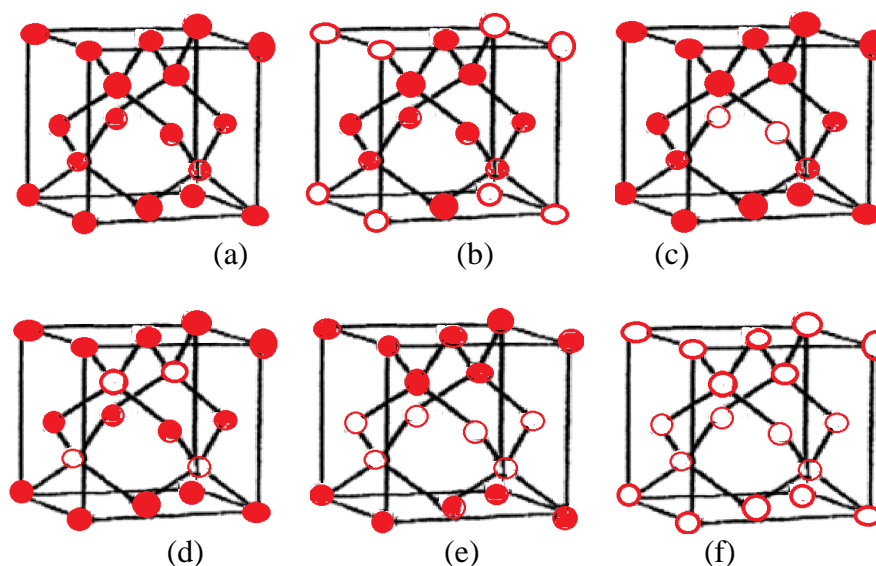


Figure 1. (a) $\text{LiNi}_{0.5}\text{Mn}_{1.5}\text{O}_4$, (b) $\text{Li}_{0.875}\text{Ni}_{0.5}\text{Mn}_{1.5}\text{O}_4$ with diagonal Li vacancy, (c) $\text{Li}_{0.875}\text{Ni}_{0.5}\text{Mn}_{1.5}\text{O}_4$ with opposite Li vacancy, (d) $\text{Li}_{0.5}\text{Ni}_{0.5}\text{Mn}_{1.5}\text{O}_4$ with Li vacancy become ABABABAB arrangement along (111) surface, (e) $\text{Li}_{0.5}\text{Ni}_{0.5}\text{Mn}_{1.5}\text{O}_4$ with Li vacancy become ABABABAB arrangement along (110) surface, (f) $\text{Ni}_{0.5}\text{Mn}_{1.5}\text{O}_4$ with no lithium. ● represents Li ion, ○ represents Li vacancy.

In this study, we used the CASTEP code (Materials Studio package) to complete the calculation. In order to make the calculation converge, we neglected the 10% Li/Mn site disorder. The initial crystal model was built base on the experimental lattice parameters and ionic positions [18]. The

generalized gradient approximation (GGA and GGA+U) was applied to deal with the exchange correlation potential [19]. Both the Hubbard U value of Mn and Ni atom are set as 5.0. In order to relax the structures of the model, we proceeded the geometry optimization firstly. Then, we used the relaxed structures to calculate the total energies and the electronic structures without changing the energy cut-off and k-points in the geometry optimization. The convergence tests of the total energy with respect to the k-points sampling and cut-off energy have been carefully examined. The final set of energies was computed with an energy cut-off of 500 eV and integration using 6×6×6 k-point sampling over the supercell irreducible Brillouin zone, generated by the Monkhorst-Pack scheme [20]. The total energy, self-consistent field (SCF) and root-mean-square (RMS) displacement of atoms were converged within 10^{-4} , 2×10^{-6} eV and 0.001 °Å, respectively. RMS force on atoms and RMS stress tensor were set to 0.05 eV/°Å and 0.1 Gpa. Before the calculations, the ionic positions and the lattice parameters were fully relaxed firstly. The final force was within 0.01eV/Å on each atom. We chose Gaussian smearing method with a smearing width of 0.01 eV to calculate the density of states (DOS) finally. In order to study the structural characteristics of $\text{Li}_{1-x}\text{Ni}_{0.5}\text{Mn}_{1.5}\text{O}_4$, we only took the neutral defects into consideration and constructed 6 models as shown in Fig. 1.

In this paper, sol-gel self-combustion method was used to prepare the $\text{LiNi}_{0.5}\text{Mn}_{1.5}\text{O}_4$ material. The galvanostatically charge-discharge tests is used to evaluate the electrical properties of the electrode material. The current is set according to the theoretical specific capacity of the electrode material, the quality of the active material on the electrode and magnification test. Charge-discharge tests were performed galvanostatically at a current rate of 0.1 C with cut-off voltages of 3.5--4.8 V at room temperature in this study.

3. RESULTS AND DISCUSSION

3.1 Structure of $\text{Li}_{1-x}\text{Ni}_{0.5}\text{Mn}_{1.5}\text{O}_4$ ($P4_332$)

The first charge-discharge curves and the cycle performances of $\text{LiNi}_{0.5}\text{Mn}_{1.5}\text{O}_4$ have been researched. From the research, we find that the charge and discharge specific capacity of the $\text{LiNi}_{0.5}\text{Mn}_{1.5}\text{O}_4$ with Fd-3m space group was 119.45 mAhg⁻¹ and 112.44 mAhg⁻¹, respectively. The charge and discharge specific capacity of the $\text{LiNi}_{0.5}\text{Mn}_{1.5}\text{O}_4$ with $P4_332$ space group was 100.26 mAhg⁻¹ and 90.23 mAhg⁻¹, respectively, while the value is 85.70 mAhg⁻¹ and 79.21 mAhg⁻¹ in the reference [21], indicating that the sol-gel self-combustion method is better than high temperature synthesis method for preparing $\text{LiNi}_{0.5}\text{Mn}_{1.5}\text{O}_4$. The discharge capacity of the Fd-3m and $P4_332$ space group was reduced to 91.05 mAhg⁻¹ and 81.07 mAhg⁻¹ after 20 cycles [22]. This is mainly because of the Jahn-Teller active. Mn-3d_{z²} orbitals were filled with electrons, then the original five-degenerate Mn-3d orbital split into triple degenerate t_{2g} state (d_{xy}, d_{yz} and d_{xz}) and double degenerate e_g states (d_{x²-y²} and d_{z²}), namely JT effect [23].

It can be found that the structure of the $P4_332$ space group is more stable than the Fd-3m space group from the above analysis, therefore, the $P4_332$ space group is chosen as the initial structure of $\text{Li}_{1-x}\text{Ni}_{0.5}\text{Mn}_{1.5}\text{O}_4$. In order to study the structural characteristics of $\text{Li}_{1-x}\text{Ni}_{0.5}\text{Mn}_{1.5}\text{O}_4$, we only considered

neutral defects, and constructed six models as shown in Figure 1. For $\text{Li}_{1-x}\text{Ni}_{0.5}\text{Mn}_{1.5}\text{O}_4$, 8c sites are located by Li ions, and 12d and 4a sites are occupied by Mn ions and Ni ions, respectively, and O ions are distributed in the 8c and 24e sites [24]. Table 1 shows the lattice parameters, volume and bond length of $\text{Li}_{1-x}\text{Ni}_{0.5}\text{Mn}_{1.5}\text{O}_4$ after relaxation. The structure of $\text{Li}_{1-x}\text{Ni}_{0.5}\text{Mn}_{1.5}\text{O}_4$ has changed, and the lattice parameter decreased from 8.342 Å to 8.247 Å with the decrease of Li content. But the change in each direction is the same, so the octahedral structure is unchanged in the process of de-lithium, which indicating that the structure of $\text{Li}_{1-x}\text{Ni}_{0.5}\text{Mn}_{1.5}\text{O}_4$ is very stable [25, 26]. The length of Ni-O and Mn-O bonds decreases with the increase of de-lithium. The Mn-O bond decreases from 2.101 Å to 1.911 Å, while the Ni-O bond decreases from 2.065 Å to 1.965 Å.

Table 1. Lattice parameters, volume and bond length of $\text{Li}_{1-x}\text{Ni}_{0.5}\text{Mn}_{1.5}\text{O}_4$ (P4₃32)

Chart	Fig. 1. (a)	Fig. 1. (b)	Fig. 1. (c)	Fig. 1. (d)	Fig. 1. (e)	Fig. 1. (f)
$\text{Li}_{1-x}\text{Ni}_{0.5}\text{Mn}_{1.5}\text{O}_4$	$\text{LiNi}_{0.5}\text{Mn}_{1.5}\text{O}_4$	$\text{Li}_{0.875}\text{Ni}_{0.5}\text{Mn}_{1.5}\text{O}_4$	$\text{Li}_{0.875}\text{Ni}_{0.5}\text{Mn}_{1.5}\text{O}_4$	$\text{Li}_{0.5}\text{Ni}_{0.5}\text{Mn}_{1.5}\text{O}_4$	$\text{Li}_{0.5}\text{Ni}_{0.5}\text{Mn}_{1.5}\text{O}_4$	$\text{Ni}_{0.5}\text{Mn}_{1.5}\text{O}_4$
x	0	1/8	1/8	1/2	1/2	1
a (Å)	8.342	8.329	8.329	8.286	8.304	8.247
V (Å ³)	580.471	577.837	577.848	568.959	570.098	560.818
Mn-O (Å)	2.101	1.965	1.965	1.965	1.965	1.911
Ni-O (Å)	2.065	2.016	2.016	1.960	1.961	1.965

3.2 The voltage of $\text{Li}_{1-x}\text{Ni}_{0.5}\text{Mn}_{1.5}\text{O}_4$ (P4₃32)

In order to improve the energy density of $\text{LiNi}_{0.5}\text{Mn}_{1.5}\text{O}_4$ (P4₃32), and enhance rechargeable voltage when lithium emerge from the cathode, we calculated the intercalation voltage using first-principles. It can be represented by [27]

$$V_{\text{ave}} = -\Delta G/nF \quad (1)$$

Where ΔG is the change in Gibbs free energy for the intercalation reaction, F is the Faraday constant, n represents the delithiated amount. It is assumed that the reaction volume and entropy change are very small. Thus, the average intercalation voltage can be approximated given by internal energy ΔE :

$$V_{\text{ave}} = -\Delta E/nF \quad (2)$$

Where ΔE is the difference of total energies of $\text{Li}_{1-x}\text{Ni}_{0.5}\text{Mn}_{1.5}\text{O}_4$ (P4₃32) and $\text{LiNi}_{0.5}\text{Mn}_{1.5}\text{O}_4$ (P4₃32). The theoretical and experimental values of voltage were shown as table 2. The total energy decrease from -28731.220 eV to -27178.422 eV, and the voltage decreased from 4.7 V to 4.3 V with the reduction of Li amount. The theoretical values at variance with the experimental values is due to the generalized gradient approximation. It has been speculated that this difference come from the generalized gradient approximation overestimation the binding energy of Li. It should be considered that the voltage does not include the contribution of the surface of positive electrode material, the kinetic energy or thermal entropy. All the formation energy of $\text{Li}_{1-x}\text{Ni}_{0.5}\text{Mn}_{1.5}\text{O}_4$ (P4₃32) is negative,

which display that the structure of crystal is stable with no phase separation, which is consistent with the reference [28].

Table 2. Total energy, formation energy and voltage of $\text{Li}_{1-x}\text{Ni}_{0.5}\text{Mn}_{1.5}\text{O}_4$ (P4₃32)

Chart	Fig. 1. (a)	Fig. 1. (b)	Fig. 1. (c)	Fig. 1. (d)	Fig. 1. (e)	Fig. 1. (f)
$\text{Li}_{1-x}\text{Ni}_{0.5}\text{Mn}_{1.5}\text{O}_4$	$\text{LiNi}_{0.5}\text{Mn}_{1.5}\text{O}_4$	$\text{Li}_{0.875}\text{Ni}_{0.5}\text{Mn}_{1.5}\text{O}_4$	$\text{Li}_{0.875}\text{Ni}_{0.5}\text{Mn}_{1.5}\text{O}_4$	$\text{Li}_{0.5}\text{Ni}_{0.5}\text{Mn}_{1.5}\text{O}_4$	$\text{Li}_{0.5}\text{Ni}_{0.5}\text{Mn}_{1.5}\text{O}_4$	$\text{Ni}_{0.5}\text{Mn}_{1.5}\text{O}_4$
Total energy (eV)	-28731.220	-28536.757	-28536.772	-27954.176	-27954.138	-27178.422
Formation energy (eV)	-	-4.419	-4.404	-16.868	-16.906	-32.446
Theoretical voltage(V)	4.70	4.69	4.67	4.48	4.49	4.3
Experimental Voltage (V)	4.68[2] 4.70[5]	4.68	4.68	4.65	4.65	4.60

3.3 Capacity of $\text{Li}_{1-x}\text{Ni}_{0.5}\text{Mn}_{1.5}\text{O}_4$ (P4₃32)

Table 3. Theoretical capacity and experimental capacity of $\text{Li}_{1-x}\text{Ni}_{0.5}\text{Mn}_{1.5}\text{O}_4$ (P4₃32)

Chart	Fig. 1. (a)	Fig. 1. (b)	Fig. 1. (c)	Fig. 1. (d)	Fig. 1. (e)	Fig. 1. (f)
$\text{Li}_{1-x}\text{Ni}_{0.5}\text{Mn}_{1.5}\text{O}_4$	$\text{LiNi}_{0.5}\text{Mn}_{1.5}\text{O}_4$	$\text{Li}_{0.875}\text{Ni}_{0.5}\text{Mn}_{1.5}\text{O}_4$	$\text{Li}_{0.875}\text{Ni}_{0.5}\text{Mn}_{1.5}\text{O}_4$	$\text{Li}_{0.5}\text{Ni}_{0.5}\text{Mn}_{1.5}\text{O}_4$	$\text{Li}_{0.5}\text{Ni}_{0.5}\text{Mn}_{1.5}\text{O}_4$	$\text{Ni}_{0.5}\text{Mn}_{1.5}\text{O}_4$
Theoretical capacity (mAhg ⁻¹)	146	127.7	127.7	73	73	0
Experimental capacity (mAhg ⁻¹)	90.23	78.95	78.95	45.12	45.12	0

Theoretical capacity of battery is the maximum theoretical value obtained by calculating the amount of substance according to Faraday's law, which can be defined as [29]

$$c = 6.023 \times 10^{23} \times 1.6022 \times 10^{-19} \times n_0 \times \frac{m_0}{F_w} \div 3600$$

$$= \frac{26.8n_0m_0}{F_w} \tag{3}$$

where m_0 is the amount of the complete reaction active substance, F_w is the molecular weight of active substance, n_0 is the number of electrons. From equation (3), we can quickly get the theoretical capacity. The theoretical and experimental capacity as shown in table 3. Table 3 demonstrated that the theoretical capacity reduced from 146 mAhg⁻¹ to 0 with the increase of delithiated amount or Li/Mn molar ratio [30]. We can see from the table that the theoretical capacity is larger than the experimental

capacity, which due to the existence of the crystal thermal movement, as well as the unsuitable temperature and air in the preparation process, that affect the arrangement of atoms, resulting the experimental crystal structure can not be as regular as the ideal structure. It is need to be emphasized that these defects has a great impact on the crystal performance.

4. CONCLUSIONS

The crystal structure, voltage and capacity of $\text{Li}_{1-x}\text{Ni}_{0.5}\text{Mn}_{1.5}\text{O}_4$ were studied by using the first principle theory. The results show that the structure of $\text{Li}_{1-x}\text{Ni}_{0.5}\text{Mn}_{1.5}\text{O}_4$ has changed, and the lattice parameter decreased from 8.342 Å to 8.247 Å with the decrease of Li content but the octahedral structure is unchanged in the process of de-lithium. The length of Ni-O and Mn-O bonds decreases with the increase of de-lithium. The Mn-O bond decreases from 2.101 Å to 1.911 Å, while the Ni-O bond decreases from 2.065 Å To 1.965 Å. The total energy decrease from -28731.220 eV to -27178.422 eV, and the voltage decreased from 4.7 V to 4.3 V with the reduction of Li amount. All the formation energy of $\text{Li}_{1-x}\text{Ni}_{0.5}\text{Mn}_{1.5}\text{O}_4$ (P4₃32) is negative, which display that the structure of crystal is stable with no phase separation. The theoretical capacity reduced from 146 mAhg⁻¹ to 0 with the increase of delithiated amount or Li/Mn molar ratio.

ACKNOWLEDGEMENTS

This project was supported by the Fund and Opening Project of Guangxi Key Laboratory of Automobile Components and Vehicle Technology, Guangxi University of Science and Technology (No.15-A-03-01, 2015KFZD02). And it was financially supported by the research of Based on Science and Technology Plan of Guangdong Province (2015A010105026). We gratefully acknowledge support from Dr. Tang Fawei in the computing.

References

1. G. Jia, C. Jiao, W. Xue, S. Zheng, J. Wang, *Solid State Ionic*, 292 (2016) 15.
2. S.E. Khakani, D. Rochefort, D.D. Macneil, *J. Electrochem. Soc.*, 163 (2016) 947.
3. O. Sha, S.L. Wang, Z. Qiao, W. Yuan, Z.Y. Tang, *Mater. Lett.*, 89 (2012) 251.
4. X. Fang, M. Ge, J. Rong, C. Zhou, *J. Mater. Chem. A*, 12 (2013) 4083.
5. J.C. Fang, Y.F. Xu, G.L. Xu, S.Y. Shen, J.T. Li, *J. Power Sources*, 304 (2016) 15.
6. Y. Xue, Z. Wang, F. Yu, Y. Zhang, G. Yin, *J. Mater. Chem. A*, 12 (2014) 4185.
7. N.K. Yavuz, A. Bhaskar, D. Dixon, M. Yavuz, K. Nikolowski, *J. Power Sources*, 267 (2014) 533.
8. P.P. Prosini, M. Carewska, G. Tarquini, F. Maroni, A. Birrozzi, *Ionics*, 22 (2015) 515.
9. I. Kishida, K. Orita, A. Nakamura, Y. Yokogawa, *J. Power Sources*, 241 (2013) 1.
10. A. Karim, S. Fosse, K.A. Persson, *Phys. Rev. B: Condens. Matter*, 87 (2013) 22.
11. Q.S. Song, H.T. Yu, Y. Xie, T.F. Yi, Z.C. Xiong, *Ionics*, 12 (2016) 1.
12. E. Hu, S.M. Bak, J. Liu, X. Yu, Y. Zhou, *Chem. Mater.*, 26 (2013) 1108.
13. M. Mancini, P. Axmann, G. Gabrielli, M. Kinyanjui, U. Kaiser, *Chem.*, 14 (2016) 1843.
14. A. Vanchiappan, A. Nagasubramanian, S. Nageswaran, *Electrochim. Acta*, 215 (2016) 647.
15. L.Y. Liu, S.H. Tao, *J. Mol. Sci.*, 20 (2012) 81.
16. J. Shi, Z. Wang, Y.Q. Fu, *J. Mater. Sci. Lett.*, 52 (2017) 605.
17. Y.J. Gu, Y. Li, Y.B. Chen, H.Q. Liu, *Electrochim. Acta*, 213 (2016) 368.
18. Y. Li, Y.J. Gu, Y.B. Chen, H.Q. Liu, J.X. Ding, *Mater. Lett.*, 180 (2016) 105.
19. J. Cheng, X. Li, Z. Wang, H. Guo, *Ceram. Int.*, 42 (2016) 3715.

20. L.L. Xiong, Y.L. Xu, C. Zhang, *J. Solid State Electrochem.*, 15 (2011) 1263.
21. X.H. Liang, L. Shi, Y.S. Liu, *Adv. Mater. Res.*, 863 (2014) 956.
22. X.H. Liang, M.H. Huang, *Int. J. Electrochem. Sci.*, 11 (2016) 4611.
23. H. Seyyedhosseinzadeh, F. Mahboubi, A. Azadmehr, *Electrochim. Acta*, 108 (2013) 867.
24. D. Liu, J. Han, J.B. Goodenough, *J. Power Sources*, 9 (2010) 2918.
25. N. Hayakawa, T. Kawai, H. Sakai, A. Honda, T. Oyama, K. Yamanaka, *J.surf.sci.soc.jpn*, 34 (2013) 415.
26. H.X. Liang, R.X. Jiang, L. Xiao, H.X. Liu, *Appl. Compos. Mater.*, 44 (2011) 2259.
27. X. Zhao, Y. Cui, X. Liang, *Solid State Ionics*, 192 (2011) 321.
28. M. Mancini, P. Axmann, G. Gabrielli, M. Kinyanjui, U. Kaiser, *Chem.*, 9 (2016) 1843.
29. X.G. Xin, J.Q. Shen, S.Q. Shi, *Chin. Phys. B*, 21 (2012) 128202.
30. M. Mamiya, K. Tokiwa, J. Akimoto, *J. Power Sources*, 310 (2016) 12.

© 2017 The Authors. Published by ESG (www.electrochemsci.org). This article is an open access article distributed under the terms and conditions of the Creative Commons Attribution license (<http://creativecommons.org/licenses/by/4.0/>).